ISSN: 2348 - 2117

International Journal of Engineering Technology and Computer Research (IJETCR)
Available Online at www.ijetcr.org
Volume 3; Issue 5; September-October-2015; Page No. 78-89

Aquifer Hydraulic Parameters Estimation from Surface Geoelectrical Measurements in Wadi Al Hawad Basin, Sudan

Nasreldin H. Abdalla[1], Nuha E. Mohamed[2]

[1] General Service Agency (GSA), GSA Regional Office for Africa, Kenya

nasrhamed25@yahoo.com

[2]Faculty of Petroleum and Minerals - Al Neelain University - Sudan

nuhazein@hotmail.com

Abstract

The relationship between hydraulic parameters and electric resistivity is one of the most difficult and challenging approaches in the field of hydrogeophysics. Usually, the aquifer parameters are obtained by the analysis of pumping tests data which provide limited spatial information and turnout to be overpriced and time consuming. Vertical Electrical Soundings and pump testing of boreholes were conducted to delineate the aquifer system at Abu Deleig area in northeastern part of Khartoum basin. The electrical resistivity survey confirms the existence of two groundwater aquifers. An upper aquifer composed mainly of alluvial sediments and shallow sandstone is found at depths ranging between 20-30 m; while the lower aquifer is predominantly Cretaceous sandstone found at depths below 50 m, each of these aquifers shows a wide range of variable hydraulic parameters, due to the high in-homogeneity of the sedimentary formations. In this study the groundwater resistivities (ρ_w) were measured from boreholes samples and apparent formation factor (F_a), was estimated using formation resistivity from vertical electrical sounding, and then used to estimate the intrinsic formation factor. Intrinsic formation factor used to estimate porosity, estimated porosity was then, used in Kozeny-Carman equation to estimate hydraulic conductivity. The findings show a good match between pumped and estimated hydraulic parameters for the area where borehole information is very sparse and grain size data is not available and this an integrated approach is a good alternative to drilling more wells and conducting pump tests.

Key Words: Al Hawad, Aquifer, Parameters, Resistivity, Sudan.

1. INTRODUCTION

The arid and semi-arid regions of the world are under severe and increasing pressure due to expanding populations, groundwater becomes more important source of uncontaminated water, improved hydrogeological knowledge, new groundwater exploration technologies and data processing methods must be efficient to facilitate investigations and evaluation of the groundwater resources.

Many investigation techniques are commonly employed to estimate the spatial distribution of aquifer parameters such as hydraulic conductivity, transmissivity and aquifer depth. In areas with few pumping test information, the spatial distribution of aquifer properties cannot be confidently calculated; therefore a large effort has been under taken to explore the potential of using geophysical data to compensate for the scarcity of in situ hydrological measurements.

It was observed that the integration of aquifer parameters calculated from the existed boreholes locations and electrical parameters extracted from surface resistivity measurements can provide useful method for obtaining information on aquifer properties, since a correlation between hydraulic and electrical aquifer properties can be possible [1-7]. Several methods for integration of hydrological and geophysical data include regression models [1], kriging models, inversion models and Bayesian models [6].

Despite the difference in the methods and the geophysical data, it has been widely recognized that the most difficult part of the integration is tying hydrological measurements to geophysical data because of the scale and resolution disparity between hydrological and geophysical measurements and because of their non-unique relationships due to the uncertainty associated with field data acquisition and interpretation.

This study proposes an approach based on the normal linear regression model. The main objective is to imply hydrogeophysical relationships in Al Hawad basin, i.e. data analytical statistical links between lithological and hydrological properties on one hand (e.g. lithology, porosity, permeability) and geophysical properties (e.g.

Corresponding author: Nasreldin H. Abdalla

electrical resistivity) on the other hand. Wadi Al Hawad basin is represented by Abu Deleig area, which is located in the northeastern part of Khartoum basin.

2. GEOLOGY AND HYDROGEOLOGY

Abu Delaig is a small town some 200 km NE of Khartoum (Fig 1) lies in Wadi Al Hawad drainage basin. The study area extends between latitudes (15º.20 N to 16º.40 N) and longitudes (33º.20 E to 34º.20 E), between the Blue Nile and Atbara River and occupies the Central Butana area of Sudan. The area is drained by the Wadi Al Hawad which is considered to be an ephemeral tributary of the River Nile which joins some 20 km downstream of Shendi. This major Wadi is joined in turn by a series of smaller Khors, which are fed by monsoonal rains. Due to the population increasing growing water demands make the water resources management extremely important for sustainable development.

Wadi Al Hawad basin lies almost on the boundary between the Cretaceous Nubian sandstone and the Basement Complex [8] which is encountered at shallow depth (26 m) in wells to the south of the town. The basal Nubian sandstone at Abu Delaig is rather heterogeneous, comprising pebble beds, thin clay layers and feldspathic sands [9-11]. The Basement Complex is mainly granodiorite with some met-sediments [12] as shown in figure (1a). The interfluves areas are flat grassland with sandy soil but often with a clay matrix, which imparts a relatively impermeable surface; gravel ridges are also common near the basement/Nubian contact (Fig 2b).

In northeastern periphery of Khartoum basin (Central Butana), the structures within the Basement complex are complicated [13-14]. The landform reflects the effect of rift faulting, being developed across a series of horsts, grabens and tilted blocks, with intervening basins. The local tectonic regime of the study area is characterized by faults of NE-SW and E-W directions (Fig 1a and c). The structural analysis defined the trends of the shear and tensional fractures, which revealed that Wadi Al Hawad is the southern continuation of the Keraf Shear Zone, the N-S trending shear zone shows predominantly sinistral strike slip movements with minor reveres components [15-17]. The related minor fractures in a NE–SW direction exhibit normal faults governing the geometry of the basin.

Two groundwater aquifers systems are existed in the study area. An upper aquifer composed mainly of alluvial sediments and shallow sandstone is found at depths ranging between 20-30 m, while the lower aquifer is predominantly Cretaceous sandstone found at depths below 50 m. The seasonal streams represent the main source of groundwater recharge in the study area. Groundwater movement within the Cretaceous Sandstone aquifer shows different flow directions among which the south and northeast are the dominant (Fig 2).

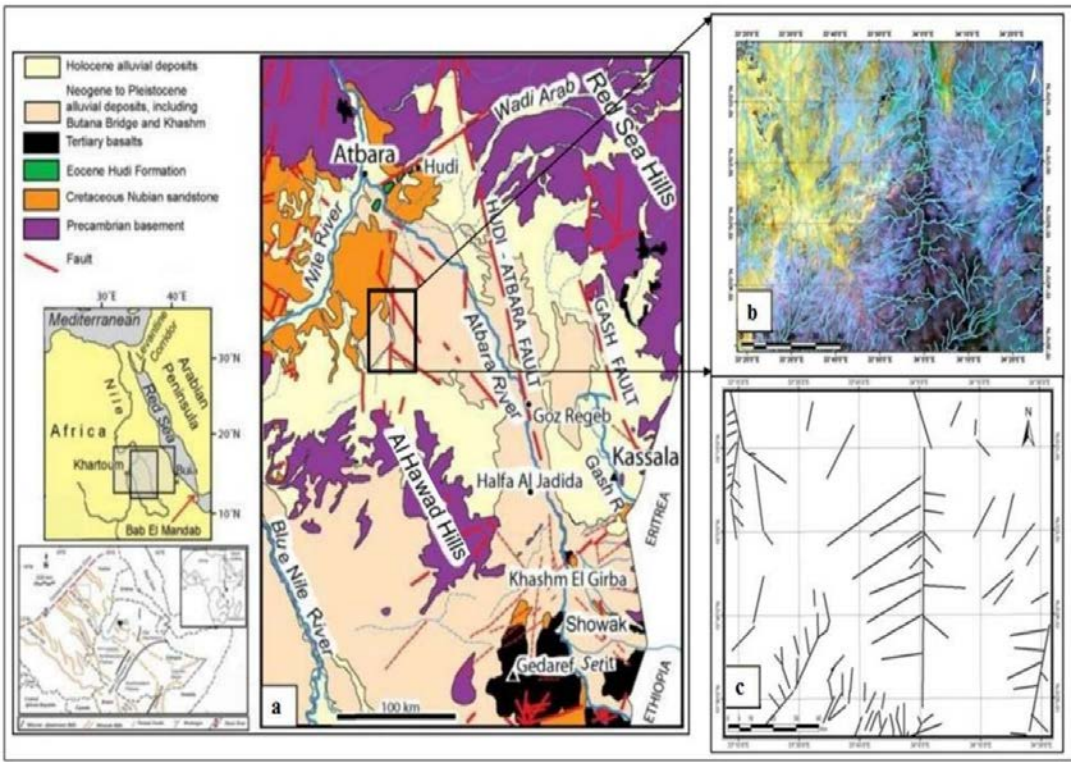

Fig. 1: Maps of the study area. (a) Location and General geological map modified after [18-19], (b) Drainage map, (c) Structural scheme of the area.

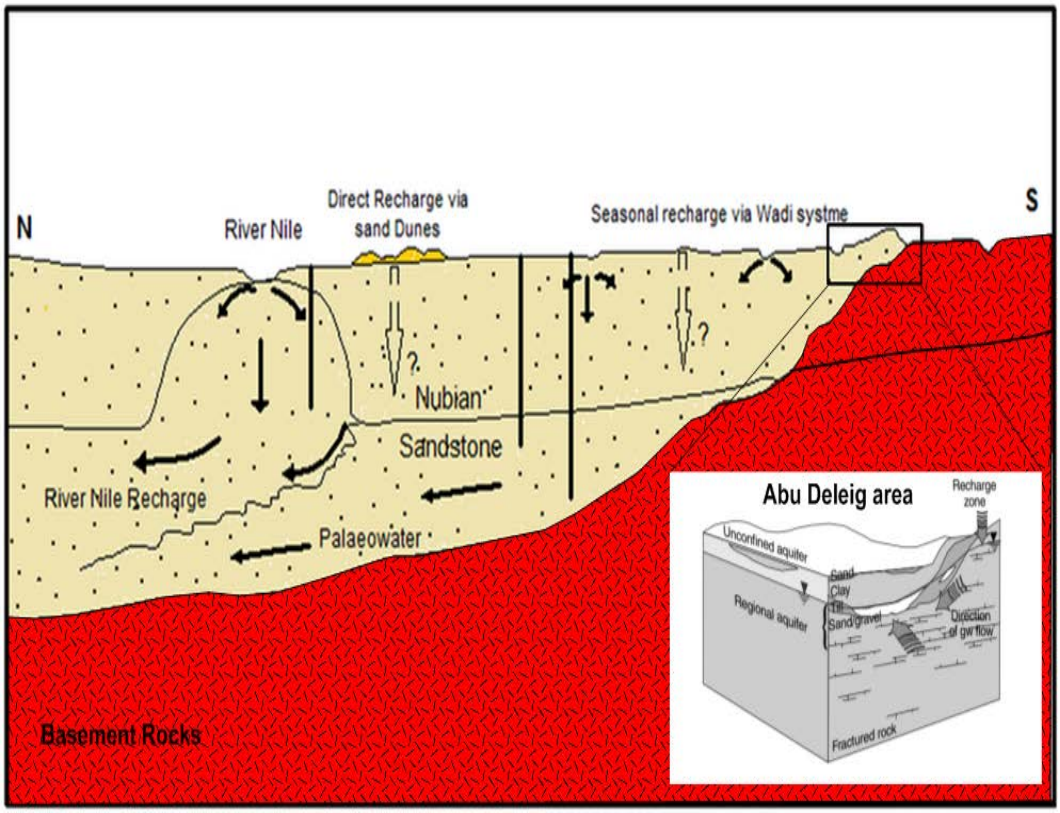

Fig. 2: Schematic Cross section, shown the main Aquifers and groundwater recharge in the study area, modified after [20].

3. METHODOLOGY AND PROCESS

A. Geoelectric Survey

Vertical Electrical Soundings (VES's) were obtained by employing a Schlumberger configuration with a half current electrode spacing (AB/2) ranging from 1.5 to 1000 m. During the current work, thirty-six of total fifty-four geoelectrical soundings (Fig. 3) have been used. All the data were collected in three phases of field work conducted respectively by the followings: Al Neelain University, the Geological Research Authority of Sudan (GRAS), and finally by some private companies. Twenty-one of the total 54 available VES measurements were selected as the most appropriate for the final modeling since they combine the low RMS error (i.e. best in quality) with the good coverage of the area of interest. The measurements were planned with the intention of covering the whole area while at the same time to be as close to the existing boreholes as possible in order to use them for calibration.

All resistivity soundings were inverted using the *IPI2Win* and *IX1D, v. 2.06* software. This package performs an automated approximation of initial resistivity model using the observed data [21]. It works in an iterative mode by calculating at the end of each step: (a) an updated model of layer thickness and resistivity and (b) the misfit function between observed and calculated data. All extracted models produced a low RMS relative error of the order of 3%. The starting model used during the inversion for each of the measured VES locations, consisted of four layers over a half space and all depths were constrained again according to the nearest borehole information (aquifer thickness, water levels and electrical conductivities), lithologic logs and geologic maps.

The collected resistivity data (VES's) was converted into a three dimensional (3D) diagram for the area under investigation (Fig.4). The relatively low resistivity values ranging between (1 to 100 Ohm-m) caused by the alluvial cover and clay with a prominent zone of unsaturated sand deposits below the ground surface (top clayey soil) occurring in the eastern and southeastern parts of the study area.

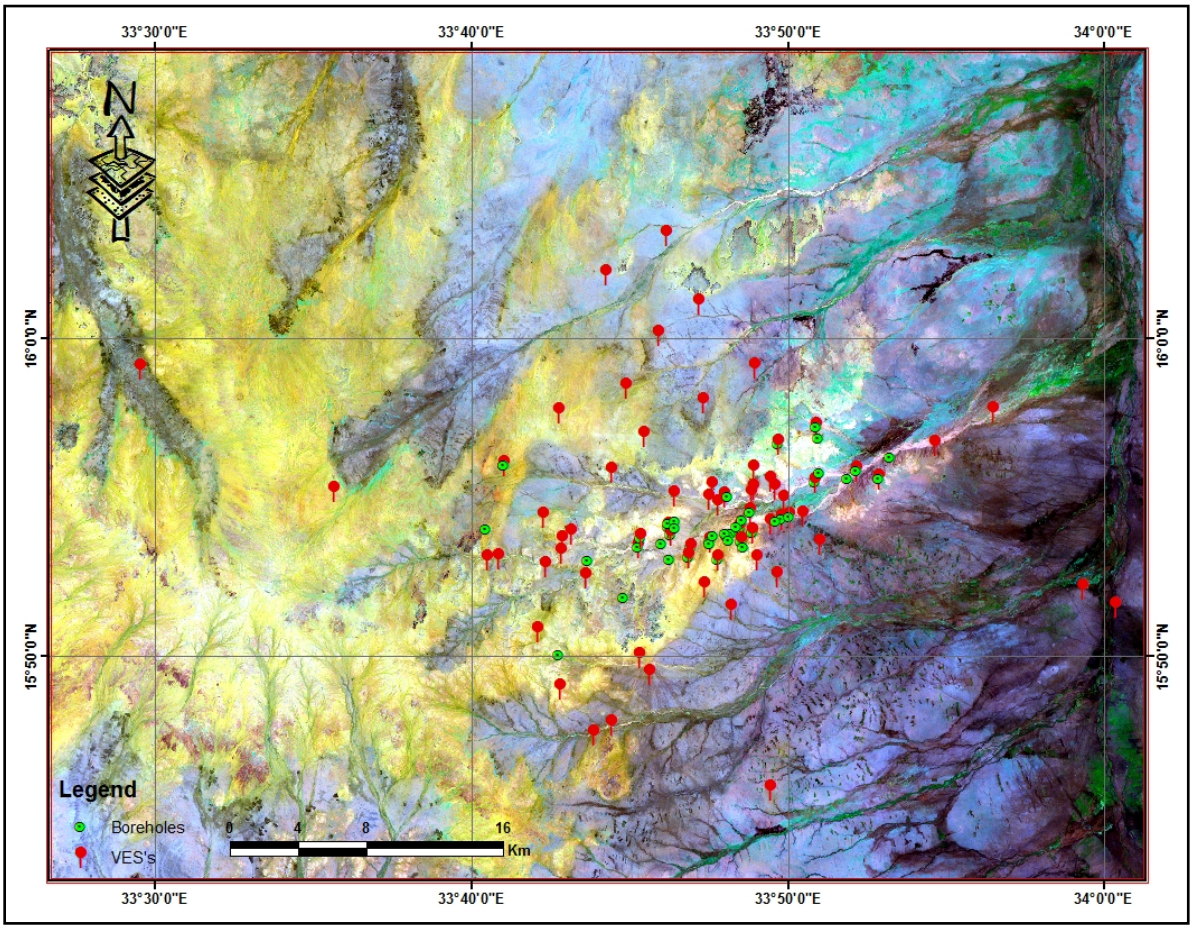

Fig. 3: Locations of the VES measurements and boreholes in the study area

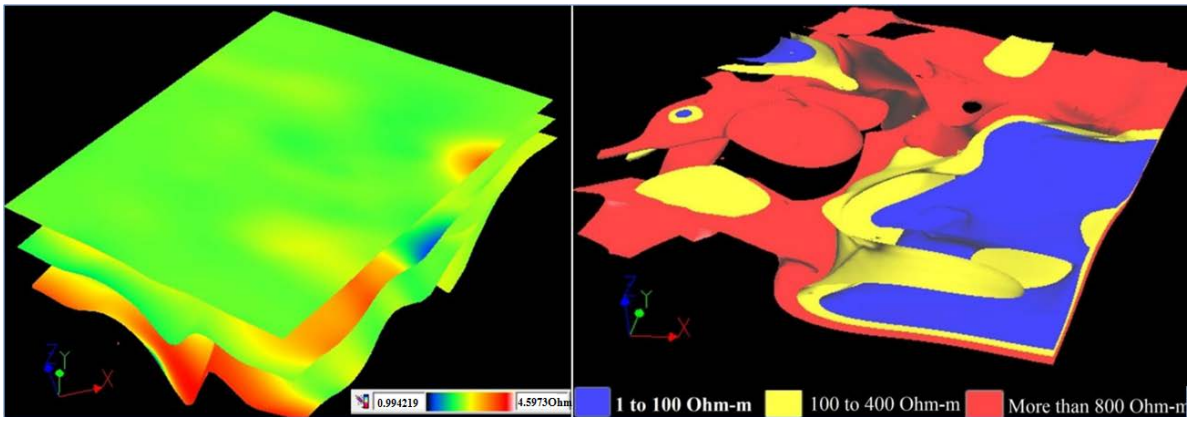

Fig. 4: 3D model obtained from resistivity values.

Below these deposits fresh water aquifer beds (Sandstone aquifer) are located. These aquifer beds are interpreted to be associated with the resistivity ranging between 100 to 400 Ωm, the aquifer is heterogeneous and consists of various sandy layers with inter bedded clays. At depths greater than 50 m in the east and southeast of the study area is interpreted as weathered basement horizon. The basement rocks are represented by high resistivity values at different depths in the area.

In the southern and southeastern parts of the area, the basement crop out at the surface and occurs at shallow depths with increasing depth towards the north and northwest by the effects of faulting. Calibration between lithologies and resistivities was done at the boreholes locations to get a unified layer model applicable to all field curves. Finally the interpretation of the resistivity and boreholes data revealed that the depth to the basement increases from 20 m at Abu Deleig in step form

to more than 400 m and extends to 40 km in NW direction in a prism-like shape with its apex occurring at Abu Deleig town.

B. Pumping Test Analysis

The most common in-situ test is the pumping test performed on wells, which involves the measurement of the rise and fall of water level with respect to time. The change in water level with time was then interpreted to arrive at aquifer parameters. Theis, Cooper and Jacob methods were used for the data analysis and calculation of the aquifer parameters, focusing on Jacob's as it is one of the most frequently used methods in pumping test analysis [22]. The pumping test data have been interpreted considering the field conditions to evaluate aquifer parameters. The location of these pumping wells is shown in figure 3.

The aquifers are characterized by average hydraulic conductivity of 8.0×10^{-3} m/min and the transmissivity (T) of 3.85×10^{2} m²/min. The groundwater in the upper aquifer is characterized by TDS of 150-1800 ppm. The water is mainly dominated by alkaline earth with calcium and magnesium increasing with the flow direction. The groundwater in the sandstone aquifer is predominantly of the chloride- calcium type that reflects deficiency of recharge [23].

C. Geoelectric versus Hydraulic Parameters

Geophysicists have realized that the integration of aquifer parameters calculated from existing borehole locations and subsurface resistivity parameters extracted from resistivity measurements can be highly effective, since a correlation between hydraulic and electrical aquifer properties can be possible as both properties are related to the pore space structure and heterogeneity.

According to Archie law [24], the resistivity of water saturated clay-free material can be described as:

$$\rho_f = \rho_w * F_i \qquad (1)$$

$$F_i = \frac{\rho_f}{\rho_w} \qquad (2)$$

Where is ρ_f is the formation resistivity, ρ_w Is the pore water resistivity being the reciprocal value of EC, which is determined on water samples taken from boreholes and wells by applying the following formula:

$$\rho_w = 10000/\mathrm{EC} \qquad (3)$$

F_i Is intrinsic formation factor, the intrinsic formation factor combines all properties of the material influencing electrical current flow like porosity Ø, pore shape, and digenetic cementation.

$$F_i = a.\emptyset^{-m} \qquad (4)$$

In order to calculate the hydraulic conductivity (K) from surface resistivity soundings, information regarding the porosity of the aquifer requested. The porosity of the aquifer has been estimated by using the Archie equation which can be reformulated [25] to the form as given in the equation:

$$\emptyset = e^{\frac{1}{m}\ln(a)+\frac{1}{m}\ln(\frac{1}{F_i})} \qquad (5)$$

Where Ø is the porosity, m is the cementation factor and a is the coefficient of lithology. The values of m and a should be determined for the site under investigation. In this study due to the lack of borehole information, this was not possible, so theoretical values in accordance with lithology have been assumed as: a = 1.0, m = 1.3 (Loose sand), and a = 0.7, m = 1.9 (Sandstone) as suggested in [26] and [27].

Many studies concluded that Archie's law breaks down in three cases: (1) clay contaminated aquifer [27-28], (2) partially saturated aquifer [4 and 29], and (3) fresh water aquifer [2]. In Archie condition (fully saturated salt water clean sand), the apparent formation factor equals the intrinsic formation factor [24].

In the study area, the aquifer system consists of clay, silt, sand and gravels, which Archie's formula is valid only for clay-free, clean, consolidated sediments, which an additional corrective step for clay conductivity is required. For this reason, the Waxman–Smits model was considered [28] as it relates the apparent and intrinsic formation factors, *Fa* (the ratio of aquifer resistivity to fluid resistivity) and *Fi*, after taking into account the shale effects. According to [27],

$$F = F_i.(1 + BQ_v\rho_w)^{-1} \qquad (6)$$

Where: Qv represents the cation-exchange capacity per unit volume and B is the parameter describing the average mobility of the cations near the grain surfaces and is related to Ø according to [27] by the equation:

$$LogQ_v = -3.65 - 2.74log\emptyset \qquad (7)$$

The parameter B varies with resistivity according to [27] by the equation:

$$B = 3.83[1 - 0.83\exp(-0.5/\rho_w)] \qquad (8)$$

By rearrange the equation (9), obtained a linear relationship between $1/F$ and ρ_w

$$1/F = 1/F_i + \left(\frac{BQ_v}{F_i}\right)\rho_w \qquad (9)$$

Where: $1/\mathrm{F}$ is the intercept of the straight line and

$\frac{BQ_v}{F_i}$ represent the gradient. Thus by plotting $1/F$ versus water resistivity ρ_w, in principle obtains a value for the intrinsic formation factor, which will subsequently enable us to estimate porosity using equation (5).

Figure (5) show $1/F$ plotted versus water resistivity ρ_w. By applying the best fitting of the data, the range of the inverse of the intrinsic formation factor F_i is calculated. The data could be easily separated in two individual groups (depending on the geological complexity of the study area) with common characteristics as is shown by the two fitted lines (two aquifers). This is obtained by applying least squares best fit of the individual subgroups of the data, and the range of the inverse of the intrinsic formation factor *Fi* is calculated as shown in Table (1). From the data set the intrinsic formation factor range between 6.38 and 46.61 as is estimated from Figure (5). The porosities (Ø) could now be determined for the two aquifers through Eq. (5) for the reported values of (*a*) and (*m*) as shown in Table (1).

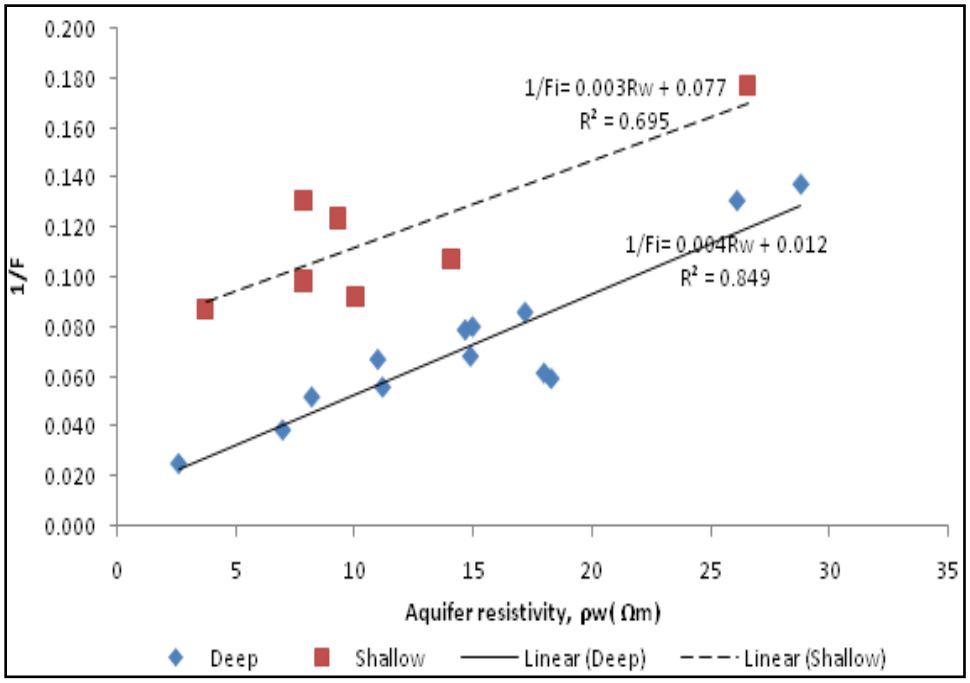

Fig.5: Cross plot between $1/F$ and fluid resistivity, ρ_w

The hydraulic conductivity (K) estimated was achieved through the use of the Kozeny - Carman equation as:

$$K = \left(\frac{\delta_{wg}}{\mu}\right).\left(\frac{d^2}{180}\right).\left[\frac{\emptyset^3}{(1-\emptyset)^2}\right] \qquad (10)$$

Where *d* is the grain size, δ_w is the water density (taken to be 1000 kg/m³), and μ is dynamic viscosity taken to be 0.0014 kg/ms [22]. The estimated hydraulic conductivity values (in m/s and in m/day) using equation (10) are shown in Table (1). The average geometrical hydraulic conductivity values for the aquifer under the investigation are 4.778 and 1.77 m/day for the shallow and deep aquifers respectively.

Table.1: Estimation of formation factor and other hydraulic parameters from the geophysical data

Site No.	Aquifer Resistivity (Ohm. m)	Bulk Resistivity (Ohm. m)	F	Aquifer Thickness (m)	Longitudinal Resistance (S)	Transverse Resistance (TR)	Porosity Ø	Hydraulic Conductivity (m/d)
1	10.06	109	10.835	20.82	2.070	209.45	0.196	3.97149
2	3.745	42.8	11.429	147	39.252	550.52	0.168	2.37211
3	7.88	79.9	10.140	29.5	3.744	232.46	0.186	3.35676
4	14.1	131	9.291	121	8.582	1706.10	0.212	5.30479
5	7.88	60	7.614	94.85	12.037	747.42	0.186	3.35676
6	26.57	150	5.645	90	3.387	2391.30	0.262	11.33816
7	9.3	75.1	8.075	72	7.742	669.60	0.192	3.74925
8	8.215	157.7	19.197	18.8	2.288	154.44	0.117	0.70948
9	14.9	218	14.631	43.6	2.926	649.64	0.150	1.60088
10	11	164	14.909	26.1	2.373	287.10	0.132	1.04099
11	18.3	308	16.831	64	3.497	1171.20	0.164	2.17984
12	18	292	16.222	161	8.944	2898.00	0.163	2.12534
13	17.2	200	11.628	60	3.488	1032.00	0.160	1.98324
14	14.68	186	12.670	109	7.425	1600.12	0.149	1.56633
15	28.818	210	7.287	43.2	1.499	1244.94	0.203	4.51609
16	11.2	200	17.857	155	13.839	1736.00	0.133	1.06699
17	26.13	200	7.654	98.1	3.754	2563.35	0.194	3.83930
18	6.99	180	25.751	114	16.309	796.86	0.110	0.58189
19	2.613	103	39.418	222	84.960	580.09	0.081	0.21967
20	14.99	187	12.475	322	21.481	4826.78	0.150	1.61511

Two of the important parameters in electrical prospecting are the longitudinal unit conductance (S, layer thickness over resistivity) and the traverse unit resistance (TR, layer thickness time's resistivity), which define the Dar Zarrouk Parameters (DZP) [30]. The DZP were also calculated for interpreted sounding layer parameters after taking into account only aquifer resistivities and its thicknesses as in equation (11):

$$S = \frac{h}{r} \qquad and \qquad TR = r.h \qquad (11)$$

Where: h is the thickness of the aquifer, and r is the resistivity of the aquifer (Ωm).

The studied aquifers system consists of fine grained, clayey-silty sand materials. Transmissivity of the studied aquifer is therefore assumed to be controlled by the thickness of the specific layer and the presence of fine/clay particles. Also, assuming that the longitudinal conductance is the dominant parameter, Equation (12) was used to calculate the Transmissivity. The constants, β and m were calculated using a linear regression taken between Transmissivity and Transverse Resistance for the fifteen locations where both data were available, Fig (6).

$$T = \beta\,(T.R)^m \qquad (12)$$

The plot of empirical relationship Eq. (12) is shown in figure (6) for the actual field data. The values of the coefficient (β) and the exponent (m) in Eq (12) is found to be β = 6.766, 1.245 and m = 0.921, 0.969 for shallow and deep aquifers respectively. The values of field data are sorted on the basis of hydraulic units one and two, the plot shows two lines with lesser scatter.

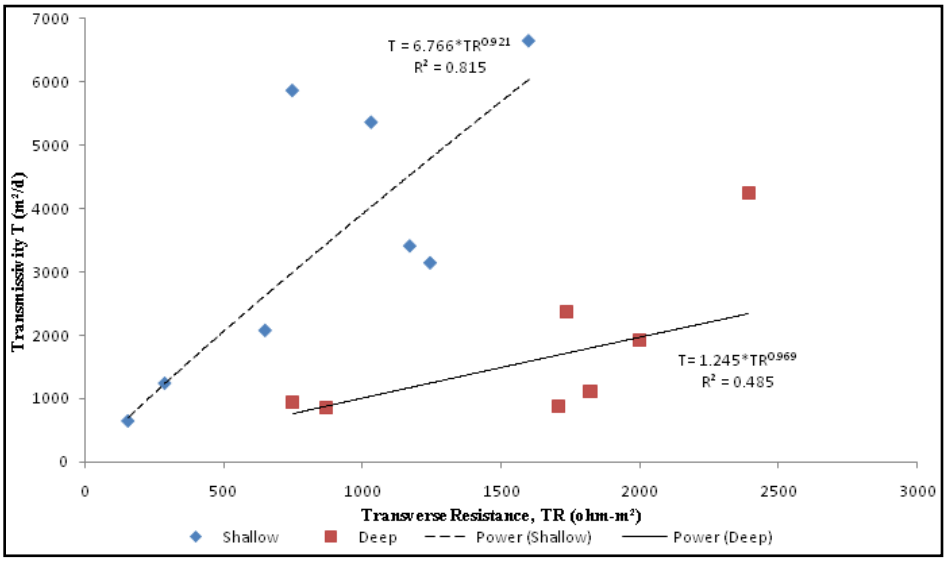

Fig. 6: Relation between Transverse Resistance, TR (Ωm²) and Transmissivity, T (m²/day).

The calculated values were compared with the observed data in Table (2) it is observed that the values computed from pumping test and generally closer to measured values in comparison to those computed from Eq. (12).
The progressive increase in both parameters suggests that the fluid potential (indicated by Transmissivity) of the aquifer in the study area, increases considerably as the transverse resistance increases. The aforementioned simultaneous change is attributed to the influence of the hydraulic and electric anisotropies, as well as to variations in lithology, mineralogy and size of grains and size and shape of the pores and pore channels.

Table 2: The calculated Transmissivity values from the geophysical data were compared with the observed Transmissivity data.

Site No.	Observed Transmissivity (m²/d)	Transverse Resistance, TR (ohm-m²)	Calculated Transmissivity (m²/d)
1	641.088	154.442	701.754
2	3142.08	1244.9376	4796.925
3	3409.92	1171.2	4534.623
4	5365.44	1032	4035.813
5	6652.8	1600.12	6044.446
6	1238.4	287.1	1242.169
7	5866.56	747.418	2998.362
8	2073.6	649.64	2635.139
9	4250.88	2391.3	2329.797
10	869.76	869.6	874.223
11	2384.64	1736	1708.226
12	1117.44	1820.353	1788.597
13	947.52	750.515	757.958
14	891.648	1706.1	1679.709
15	1926.72	2000	1959.385

4. RESULTS

The study area located in a transitional area between the Butana basement terrain to the east; and Khartoum and Shendi sedimentary basins to the west and northwest, respectively. Two type of aquifers have been recognized namely; the shallow aquifer and the deep aquifer. The

alluvial aquifers are confined to the seasonal streams; therefore, they are of limited storage capacity and small aerial extent. Each of these aquifers shows a wide range of variable hydraulic parameters, depending on pumping test, grain size analysis and due to rapid lateral and vertical changes of facies.

The calculated hydraulic parameters were interpolated with geostatistical using the kriging interpolator's technique led to a great number of artifacts, possibly because of the limited number as well as the random distribution of the available sample sites, by using this techniques, the aquifer thickness (m), transverse resistance, Transmissivity (m^2/d) and hydraulic conductivity thematic maps were created as is shown in Figures (7, 8, 9 and 10) respectively. Moreover, uncertainty analysis was applied to demonstrate the cross validation of the created maps.

The spatial maps that were derived from the interpolation of the calculated hydraulic parameters shows increasing of the aquifer thickness towards rocks of high permeability, which represent sandstone formations in northwest part of the study area (Fig 7). Due to the great thickness and relatively high permeability the lower aquifers zone may be considered quite appropriate for large-scale exploration of water.

In general there is a relation between hydraulic conductivity (Fig 8) and groundwater table depressions and salinity, drainage zones marked by low mineralized groundwater salinity. Such zones penetrate far inland from the Wadies to depressions in groundwater surface. These depressions can be explained as areas of high vertical permeability. Here the groundwater is drained to the lower part of the system where relatively high permeability occurs.

Figure 9 shows the Transmissivity distribution over the entire study area. It is clear that the highest Transmissivity values are mostly on the northwestern part of the area and some parts in the southwestern part, identifying zones of high water bearing potential. The transverse resistance is directly correlated to the Transmissivity as is shown in Figure 9 and 10. The progressive increase in both parameters suggests that the fluid potential (indicated by Transmissivity) of the aquifer in the study area, increases considerably as the transverse resistance increases. Furthermore, a relation between the estimated and presented hydraulic parameters as shown in Figures (7 to 10) and tectonic structures seems to exist with faults acting as boundaries even between the same hydro-lithological units, and define the place where aquifer parameters varies.

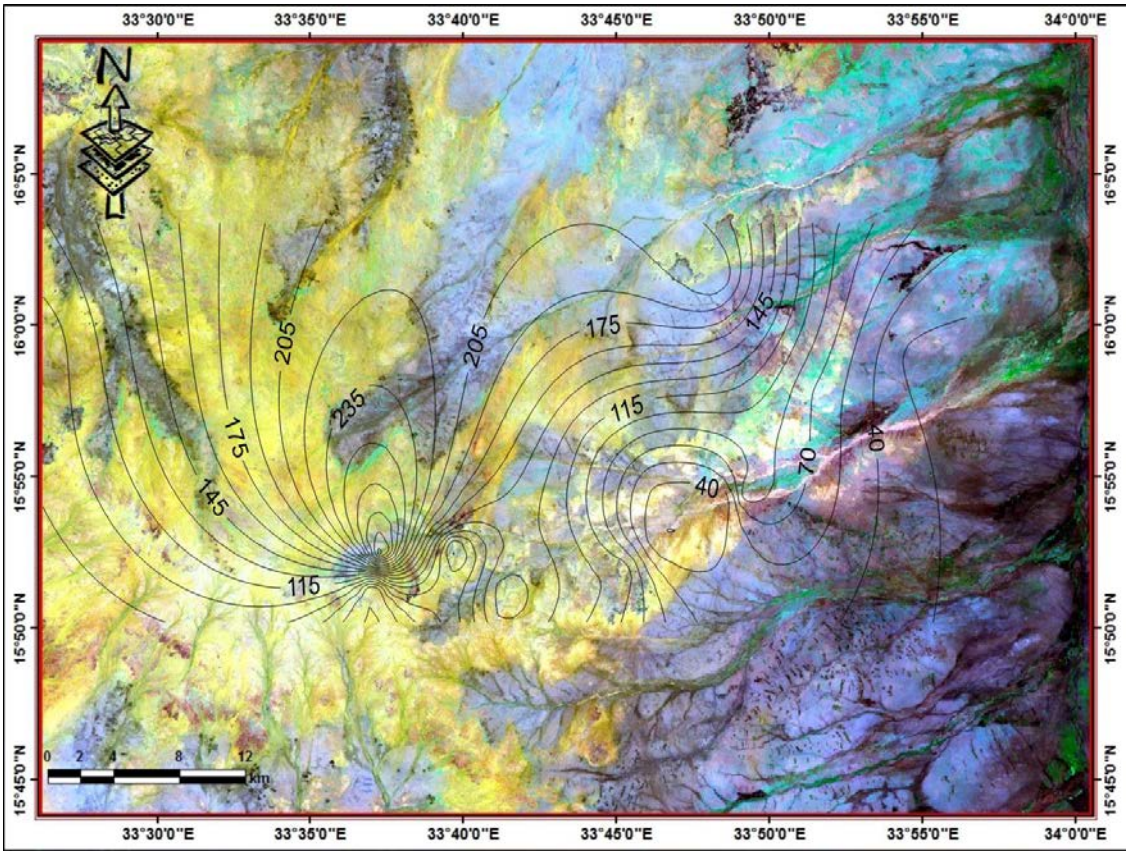

Fig. 7: The Aquifer Thickness (m) in the Study Area

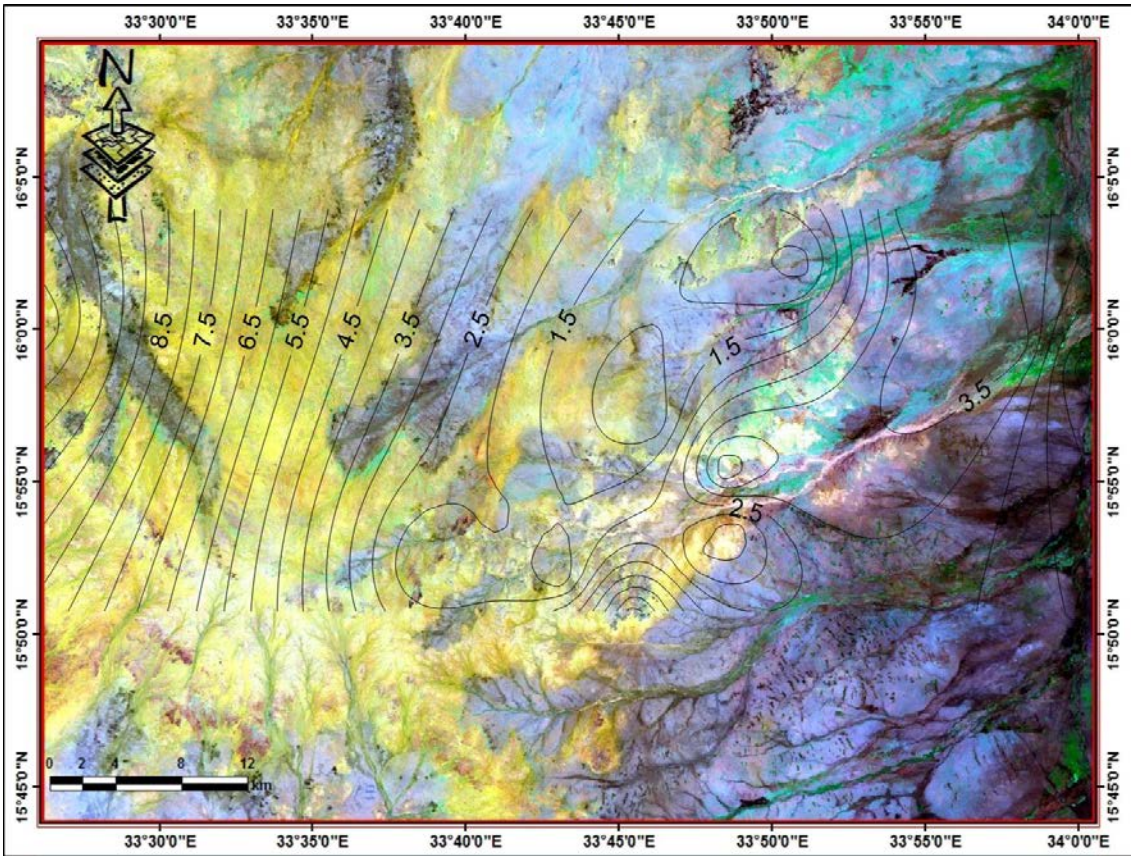

Fig. 8: Hydraulic Conductivity (m/d) Distribution in the Study Area.

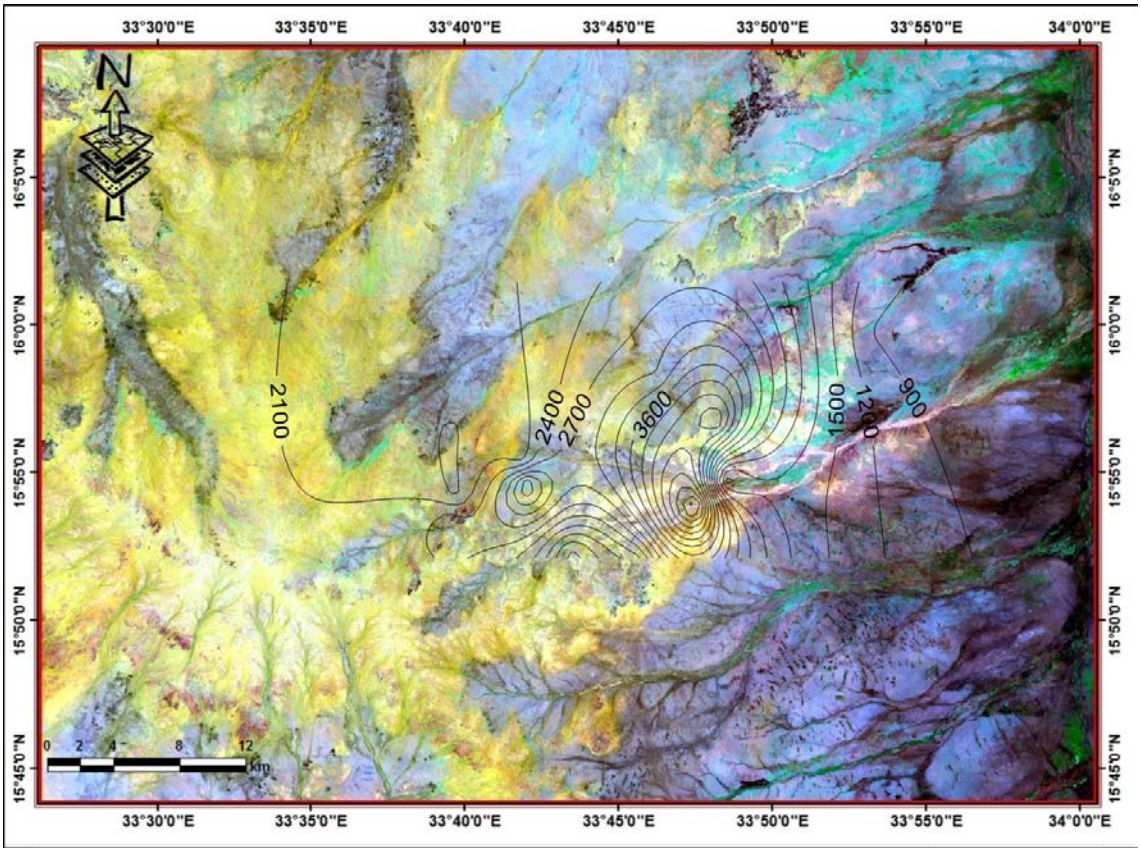

Fig. 9: Transmissivity (m^2/d) Distribution in the Study Area.

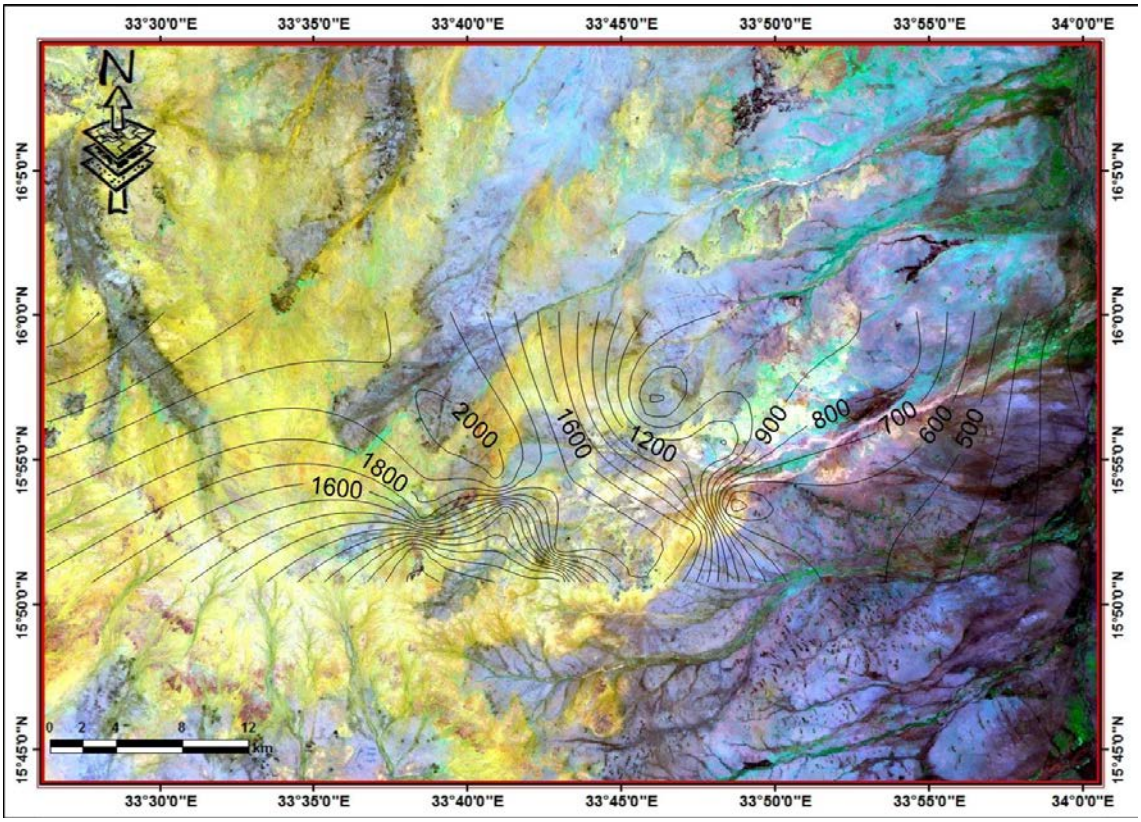

Fig. 10: Transverse Resistance Distribution in the Study Area

5. CONCLUSION

Studying the relationship between hydraulic parameters and electrical resistivity is one of the most interesting objects in both geophysics and hydrogeology. An integrated approach of estimating aquifer parameters from electrical resistivity and pumping test is a cost-effective alternative and provide a useful estimation of the aquifers parameters with varying lithological units.

The spatial maps that were derived from the interpolation of the calculated hydraulic parameters show increased aquifer thickness towards rocks of high permeability, which represent sandstone formations to northwest part of the study area. Aquifer transverse resistance and Transmissivity also seem to be spatially related with the high permeability formations mentioned above. Moreover, the increased Transmissivity in the northwest part of the study area identifies the zones of high potential within the water-bearing formations. The depression in groundwater table in some places can be explained as areas of higher vertical permeability, which the groundwater drained to the lower part of the system where relatively high permeability's occur.

Finally the estimation of hydraulic parameters from electric resistivity measurements provides the following advantages:

a. A new and important hydrogeological trend for the application of resistivity measurements and thus a prospective estimation of many hydraulic parameters through hydraulic conductivity.

b. An Evaluation of the groundwater potentiality of new reclaimed areas before well drilling. This gives advantage to select the most productive zones for new drillings.

c. Use of indirect and minimally invasive data from geoelectric measurements.

d. The accuracy of the results depends on the spatial distribution of the data which can be controlled through appropriate field survey design.

6. REFERENCES

1. Kelly, W. E., 1977. Geoelectric sounding for estimating hy-draulic conductivity.Ground Water, 15(6), 420– 425.
2. Huntley, D., 1987. Relations between permeability and electrical resistivity in granular aquifers. *Groundwater*. 24 (4): 466-474.
3. Mazac, O., Cislerova, M., & Vogel, T., 1988. Application of geophysical methods in describing spatial variability of saturated hydraulic conductivity in the zone of aeration. Journal of Hydrology, 79, 1–19.
4. Börner F.D., Schopper J.R., Weller A., 1996. Evaluation of transport and storage properties in the

soil and groundwater zone from induced polarization measurements.

5. Christiansen, A.V. and Sorensen, K., 2006 b. A survey of current trends in near-surface electrical and electromagnetic methods, *Geophysics*, 71, 5, G249-G260.
6. Rubin, Y., and S. Hubbard, 2005. Stochastic forward and inverse modeling: the hydrogeophyiscal challenge, *Water Science and Technology Library*, Springer, 487-511.
7. Niwas, S., Gupta, P. K., & de Lima, O. A. L. (2006). Nonlinear electrical response of saturated shaly sand reservoir and its asymptotic approximations. Geophysics, 71(3), 129– 133.
8. Ahmed, F. 1968. The geology of the Jebel Qeili, Butana and Jebel Sileitaat- Es-Sufr igneous complex, Nile valley, Central Sudan. Unpublished M.Sc. thesis, Univ. Khartoum.
9. Whiteman, A.J. 1971. The Geology of the Sudan Republic. Oxford University Press, UK.
10. Vail, J.R., 1988. Tectonic and Evolution of the Prot erozoic Basement of Northeastern Africa. In El Gaby, S. and Greiling, R.O. (eds). The Pan-African belt of northeast Africa and adjacent areas. *Frieder Veiwing and Sohn* (Wiesbaden), 195-226.
11. Iskander, W., Ahmed, A. A., Mokhtar, A. and Fadle, A. S., 1993. Appraisal of mineral and water resources of central Butana, Eastern region-Sudan, *ADS*, unpublished. Rep., 102 pp.
12. Vail, J.R., 1983. Pan African crustal accretion in north east Africa. – J*ournal of Africa Earth Science*. Vol. 1. No. 3/4. 285-249; Oxford.
13. Andrew, G., 1984. Geology of Sudan. Chapter VI in J. D. Tothill, agriculture in the Sudan, pp. 84-128. Oxford University Press, UK.
14. Dawoud, A.S., A, Sadig 1987. Structural and gravity evidence for an uplifted Pan-African granulite terrain in the Sabaloka inlier, Sudan. *Journal of African Earth Sciences*. Vol. 7. No. 516. Pp.789-794.
15. Binks, RM., Fairhead JD. 1992. A plate tectonic setting of Mesozoic rifts of West and Central Africa. *Tectonophysics* 213: 141–151.
16. Ibrahim, A.E. 1993. Interpretation of Gravity and Magnetic data from Sudan. Ph.D thesis. Department of earth science, University of Leeds.
17. Bailo, T., Schandelmeier, H., Franz, G., Chih-Hsien Sun and Stern, R. J. 2003: Plutonic and metamorphic rocks from the Keraf Suture (NE Sudan): a glimpse of Neoproterozoic tectonic evolution on the NE margin of west Gondwana.v.123, p. 128 67-80.
18. GRAS, 2004. Geological map of the Sudan by the Geological Research Authority of Sudan.
19. Fairhead, J.D., 1988. Mesozoic plate tectonic reconstructions of the central South Atlantic Ocean. The role of West and Central African rift system. *Tectonophysics* 155: 181–181.
20. ACSAD, 1987. "*Estimation of aquifer recharges using geochemical techniques",* Final report of lower Atbara River basin Project: BGS Research Reports, No WD/OS/87/1.
21. Bobachev, C., 2002. IPI2Win. Windows software for an automatic interpretation of resistivity sounding data, Ph.D., Moscow State University.
22. Fetter, C.W., 1994. Applied Hydrogeology. Prentice-Hall, New Jersey, USA, 3rd edition, *ISBN*: 0 -02-336490-4.
23. Elsayed, K.A., Elsheikh, A.E.M., Abdalla, N.H. 2012. Assessment of groundwater potentiality of northwest Butana Area, Central Sudan. Nile Basin Water Science & Engineering Journal, Vol.5, Issue 2, 2012.
24. Archie G.E, 1942. The electrical resistivity log as an aid in determining some reservoir characteristics. American Institute of Mineral and Metal Engineering. Technical publication, 1442, *Petroleum Technology*, pp. 8–13.
25. Soupios, P., Kouli, M., Vallianatos, F., Vafidis, A., & Stavroulakis, G., 2007. Estimation of aquifer hydraulic parameters from surficial geophysical methods: a case study of keritis basin in Chania (Crete-Greece). Journal of Hydrology, 338, 122– 131.
26. Schön J (1996) Physical Properties of Rocks: fundamentals and principles of petrophysics. In: Helbig, K., Treitel, S., (eds) Handbook of geophysical exploration. Section I, Seismic exploration. Elsevier, Oxford
27. Worthington, P.F, 1993. The uses and abuses of the Archie equations. 1. The formation factor–porosity relationship. *Journal of Applied Geophysics* 30:215–228.
28. Vinegar H.J., Waxman M.H., 1984. Induced polarization of Shaly Sand. *Geophysics* 49(8):1267–1287.
29. Martys N.S., 1999. Diffusion in partially-saturated porous materials. Mater Struct Materiauxet Constructions. 32:555–562.
30. Millet, R., 1947. The fundamental equations of electrical prospecting. Geophysics 12, 529–556.